

Live Imaging of Neuroblast Lineages within Intact Larval Brains in *Drosophila*

Clemens Cabernard and Chris Q. Doe

Neuroblasts are the precursors of the *Drosophila* central nervous system and undergo repeated physical and molecular asymmetric cell divisions. Live imaging of neuroblast lineages within intact *Drosophila* larval brains has dramatically improved our current understanding of basic cellular processes such as the establishment of cell polarity, spindle orientation, and cytokinesis. The analysis of mutant phenotypes using live imaging can enlarge our understanding of asymmetric neuroblast division and self-renewal. Although much live neuroblast imaging is performed using green fluorescent protein only, the generation of improved fluorescent proteins has led to an increase in the use of two-color imaging. Here we present a simple protocol for isolating and imaging larval brain neuroblasts. We describe procedures for the dissection and mounting of brains from third-instar *Drosophila* larvae in explant solution and their subsequent live imaging. The method provides a close approximation to the in vivo environment and produces data with high temporal and spatial resolutions. We also discuss potential problems and pitfalls and provide examples of how this technique is used.



MATERIALS

It is essential that you consult the appropriate Material Safety Data Sheets and your institution's Environmental Health and Safety Office for proper handling of equipment and hazardous material used in this protocol.

RECIPES: Please see the end of this article for recipes indicated by <R>. Additional recipes can be found online at <http://cshprotocols.cshlp.org/site/recipes>.

Reagents

Explant solution

Add 5 μL of 0.5 M ascorbic acid (Sigma-Aldrich A4034) and 50 μL of HyClone bovine growth serum (Thermo Scientific SH3054102) to 5 mL of sterile-filtered Schneider's insect medium (Sigma-Aldrich S0146). Prepare immediately before use.

Drosophila larvae (third-instar stage), wild-type and experimental (see Discussion)

Petroleum jelly (e.g., Vaseline), preheated and liquefied on a heating block before use

Equipment

Analytical computer

We use an in-house-built 64-bit multiprocessor Windows computer with 32 GB of RAM (random-access memory), a 1.5 TB boot drive, several hot swappable 1.5 TB data drives, a fast ATI Radeon HD 4870 X2 graphics card, and a Blu-ray burner to back up data.

Blu-ray disks (50-GB) (TDK Corporation)

Adapted from *Imaging in Developmental Biology* (ed. Sharpe and Wong). CSHL Press, Cold Spring Harbor, NY, USA, 2011.

© 2013 Cold Spring Harbor Laboratory Press

Cite this article as *Cold Spring Harb Protoc*; 2013; doi:10.1101/pdb.prot078162

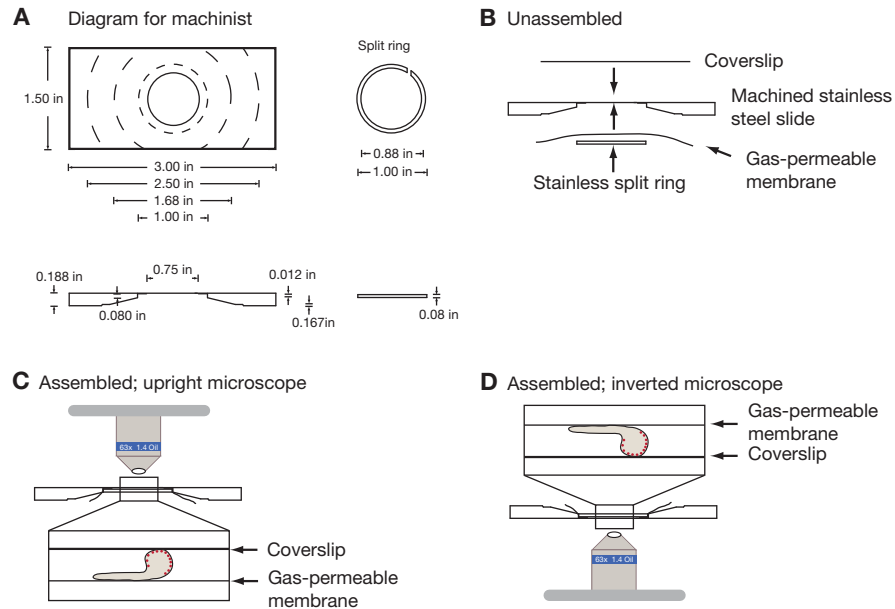


FIGURE 1. Diagram and assembly instructions of metal imaging slide. (A) Diagram of the stainless-steel slide including the split ring used for live imaging. Measurements are included to allow reproduction by a machine shop. (Reproduced, with permission of Elsevier, from Kiehart et al. [1994].) (B) Assembly order and orientation of assembled preparation on upright (C) and inverted (D) microscopes.

Confocal microscope (spinning disk or single point; equipped with 63 \times , 1.4-NA and/or 100 \times , 1.4-NA objectives)

Neuroblast live imaging can be performed using either standard single-point laser-scanning confocal systems on an upright microscope (e.g., Bio-Rad Radiance 2100; see Fig. 1C) or spinning-disk confocal systems on an inverted microscope (e.g., McBain Instruments; see Fig. 1D). For laser-scanning confocal microscopy, excite green fluorescent protein (GFP) or mCherry fluorescent proteins with 488-nm or 568-nm light, respectively, and detect emissions with standard photomultiplier tubes. Spinning-disk confocal microscopy excites the same fluorescent proteins with 488- or 561-nm lasers and detects the emission signals using an electron-multiplying charge-coupled device, Hamamatsu camera.

Dissection dishes

Heating block

Image-analysis software (e.g., ImageJ, Imaris [Bitplane], and Volocity [Improvision/PerkinElmer])

Laboratory tissue (e.g., KIMTECH Science Kimwipes; Kimberly-Clark Professional)

Membrane (gas-permeable; standard) (YSI Life Sciences 5793)

Metal imaging slide (stainless steel; machined; including split ring)

The specimens are mounted on a machined stainless-steel imaging slide, first described by Kiehart et al. (1994). The setup takes advantage of a gas-permeable membrane onto which the dissected third-instar larval brains are mounted. Assemble the machined stainless-steel metal slide (see Fig. 1A for specifications), and attach the gas-permeable membrane to the metal slide with the split ring (see Fig. 1B–D). This mounting procedure increases the viability of the specimen and allows immunohistochemistry procedures to be performed postimaging.

Micro cover glass (No. 1; 22 \times 40-mm) (VWR International 48393-048)

Paintbrush (small)

Tweezers (Dumont #5) (World Precision Instruments, Inc.)

METHOD

Larval Dissection

1. Wash 10 well-fed, third-instar, wild-type larvae in explant solution.

For this and all subsequent steps, ensure that the explant solution is warmed up to room temperature.

2. Dissect the fat bodies. Hold the mouth hooks with one set of tweezers and rupture the cuticle on one side of the larva with the other set of tweezers. The fat body will spill out into the explant solution. Transfer the dissected fat bodies with tweezers into 150 μ L of room-temperature explant solution in a separate well of a dissection dish.

Fat bodies are the source of a mitogen required for neuroblast proliferation (Britton and Edgar 1998).

3. Wash experimental larva in explant solution to remove larval food. The following method should be applied to dissect brains from experimental larvae: Using both tweezers, cutoff approximately one-third of the larva measured from the posterior spiracles. Now hold the mouth hooks of the larva with one set of tweezers. Place the other set of tweezers on the outside of the cuticle. Gently move the tweezers together. This movement will push the mouth hooks inward and inverts the cuticle. The larval brain and central nervous system (CNS) will now be facing the outside (as well as all the other tissue) and are still attached to the cuticle. Subsequently, carefully sever the axonal connections between the CNS and the cuticle until you can remove the CNS and brain from the cuticle. Leave the brain attached to the CNS. Remove as much attached tissue (imaginal discs) from the brains as possible.

4. Use tweezers to transfer the freshly dissected brains into the well containing the fat body-enriched explant solution.

Six to ten brains can be dissected in \sim 15–20 min. For best results, try to minimize the amount of time undissected larvae remain in the explant solution.

5. Transfer 135 μ L of explant solution (including fat bodies and the dissected brains) onto the membrane of the assembled metal slide (Fig. 1C,D).

It is best to mount several experimental brains; four to 10 brains are considered ideal. Roughly 10–15 fat bodies are usually transferred with the experimental brains.

Specimen Orientation and Slide Sealing

6. Position the brains close together, approximately in the middle of the membrane.

Surface tension will keep the transferred solution contained. The brains will sink to the bottom of this liquid sphere and will settle on the membrane, whereas the fat bodies will float on top.

7. Orient the brains depending on the neuroblast population to be studied (Fig. 1C,D).

To image dorsal brain neuroblasts, orient the brains with the ventral nerve cord touching the membrane and the dorsal surface of the brain lobes facing the side that will touch the cover glass (Fig. 1C,D).

8. Carefully place a cover glass on top of the explant solution, which will spread the solution over the entire membrane.

This step will most likely cause many dissected brains to lose their desired orientation.

9. Remove excess explant solution using a laboratory tissue. The optimal amount of explant solution is achieved when the brains start touching the cover glass without being squashed.

Depending on the size of the brains, the distance between specimen and cover glass can be too large. Reduce this extra space by placing a tissue at the edge of the cover glass to remove additional liquid.

See Troubleshooting.

10. If necessary, reorient the brains by moving the cover glass.

This is probably the most difficult step and requires some practice. Changing brain orientation is possible through back-and-forth movements of the cover glass. However, having several brains on the membrane will make it very difficult, if not impossible, to properly orient all specimens.

11. Once the larval brains are in the optimal orientation, immobilize the cover glass by applying preheated petroleum jelly along the edges of the coverslip with a small paintbrush.

This prevents evaporation of the explant solution and must be performed immediately after Step 10. The preparation is now ready, and imaging should not be delayed.

Image Acquisition

12. Image the specimen with a confocal or a spinning-disk (upright or inverted) microscope with the lowest laser power possible.

Because the laser power required depends on the fluorescent protein to be imaged, the levels of expression and the structure to be imaged, optimal laser power settings, gain and exposure time can only be assessed experimentally.

See Troubleshooting.

13. Acquire data. The described imaging setup will allow you to image for up to 24 h. However, increased laser exposure will result in phototoxicity. Photobleaching can also be observed, especially if imaged with high frame rates (every 5 sec or faster). Furthermore, cell-cycle length will increase over time. It is thus advisable to make a new preparation after 2 h of imaging if reliable cell-cycle measurements are the objective.

14. Process the data postacquisition as necessary or desired using your software package of choice (we use ImageJ and/or Imaris).

Processing can vary depending on data acquisition. Imaging software can be used to correct for photobleaching, change color properties, smooth images, calculate measurements, and generate four-dimensional reconstructions of the raw data.

15. Back up raw data (we use Blu-ray disks for storing raw data) and store processed data on sufficiently large data drives (we use fast 1.5 TB hard drives).

See Troubleshooting.

TROUBLESHOOTING

Problem (Step 9): Removal of explant solution creates an air bubble underneath the glass cover.

Solution: Carefully add fresh explant solution with a 20- to 100- μ L pipette tip until the bubble disappears. Remove excess liquid and reorient the brains carefully. If this happens repeatedly, it is most likely caused by an ill-fitting split ring.

Problem (Step 12): The neuroblasts do not divide, are arrested, or die.

Solution: The neuroblast cell cycle is typically 40–120 min, and mitosis (prometaphase to anaphase onset) is typically ~5–8 min. With over 200 neuroblasts per brain, there should be some neuroblasts in mitosis soon after the start of imaging. If mitoses are not observed, or if the length of mitosis is >10 min, there is a problem with the preparation. (1) The brain could have been damaged during dissection. Practice will help this. (2) The explant solution could be contaminated. Sterile filter and aliquot the Schneider's medium in 5-mL aliquots beforehand (5 mL is enough for at least one experiment, including all the washing steps), and store at 4°C. (3) The bovine growth serum used in the explant solution can lose its potency over time, and repeated thaw/freeze cycles should be avoided. Aliquot freshly purchased bovine growth serum in 50- μ L portions (50 μ L is enough for one experiment), and store at –80°C.

Problem (Step 12): There is low signal/poor image quality.

Solution: Proper mounting is critical for optimizing the detectable signal. Try removing more explant solution using the laboratory tissue technique. Optimal image quality can be achieved if the brain lobes are in direct contact with the cover glass. However, excessive removal of explant solution will squash the brains, resulting in great image quality, but potentially abnormal development. Squashed brains are easily recognized during image acquisition because the brain diameter does not change along the z-axis, whereas under optimal mounting conditions, the brain diameter will increase successively along the z-axis (starting on top).

Problem (Step 12): Bleaching occurs during image acquisition.

Solution: The most obvious solution is to reduce laser power. However, most commonly used fluorescent proteins are prone to bleaching to a certain extent. The frequency of image acquisi-

tion, even with low laser power, can cause bleaching. Thus, the only real solution is to optimize the settings for laser intensity, gain, and exposure time at the very beginning of the experiment before data collection starts. Postacquisition software can help correct for bleaching along the temporal axis of the data set.

Problem (Step 12): The neuroblast cell cycle lengthens over time.

Solution: Make a new preparation. Although dissected brains can survive for up to 24 h in explant solution, repeated exposure to laser light will slow down their cell cycle, most likely because of an accumulation of cellular toxins. If data with higher temporal resolution need to be acquired (e.g., imaging every 10 sec or less), it is advisable not to exceed imaging for >2 h with the same preparation (even if several brains are mounted but not all are imaged). In contrast, low temporal resolution will allow much longer movies to be acquired (e.g., imaging every 5 min for 12 h), although a lengthening in the cell cycle can also be observed under these conditions. For example, for a 12-h imaging experiment with the sample exposed to two lasers every 5 min, interphase can lengthen up to 8 min (C. Cabernard, unpubl.).

Problem (Step 15): There are too much data to handle and store.

Solution: A typical live-imaging experiment usually generates between 5 and 25 GB, and sometimes up to 50 GB of raw data, so careful consideration must be given to the postacquisition hardware. Buying or building a designated high-end postacquisition computer can be crucial. Make sure to generate backup copies of the generated raw data as well as all the processed images. The use of Blu-ray disks (for raw data) and hot swappable 1.5 TB data drives (for processed imaging data) as backup systems is highly recommended.

DISCUSSION

Larval neuroblasts are located very close to the surface, allowing for excellent live imaging (Fig. 2A). With some practice and the right setup, live imaging of *Drosophila* larval neuroblasts can become a standard technique for pursuing many questions previously only investigated using standard immunohistochemistry procedures. Although many previously established transgenic fly lines suitable for neuroblast live imaging are available, the choice of transgenic line must be given some thought, and proper controls should be in place.

The availability of numerous fluorescent fusion proteins and the ease with which these proteins can be expressed in a cell-type-specific manner using the Gal4/UAS system (Brand and Perrimon 1993) or by using endogenous regulatory elements facilitates live studies of neuroblast divisions (Fig. 2B). Currently, a number of suitable live-imaging markers are available that allow labeling of cellular structures such as the mitotic spindle, centrosomes, centrioles, apical and/or basal cortices, and the cleavage furrow (see Table 1 for an incomplete list). Furthermore, several Gal4 lines allow neuroblast-specific expression of fusion lines controlled by the UAS promoter (see Table 2).

Thanks to the advent of recombineering technology and homologous recombination (Venken et al. 2006, 2009; Gao et al. 2008), it is relatively easy to generate fluorescently labeled fusion proteins expressed under their native regulatory elements. Furthermore, protein trap screens provide numerous fusion proteins expressed under endogenous regulatory elements (Morin et al. 2001; Buszczak et al. 2007) such as the widely used spindle marker G147 (Morin et al. 2001), which is a protein trap in the *Jupiter* gene (Karpova et al. 2006). Recombineered protein fusions or protein trap lines are invaluable tools because the protein levels of the fusion protein closely match endogenous protein levels and are, thus, less likely to cause dominant-negative phenotypes or to show mislocalization resulting from overexpression. However, independent of the line used to label proteins or subcellular structures of interest, it is advisable to use standard immunohistochemistry procedures to ensure that increasing protein levels or adding a fluorescent tag does not alter the localization of fusion proteins. Furthermore, whenever possible, rescue experiments are recommended to test for the functionality of a generated fusion protein.

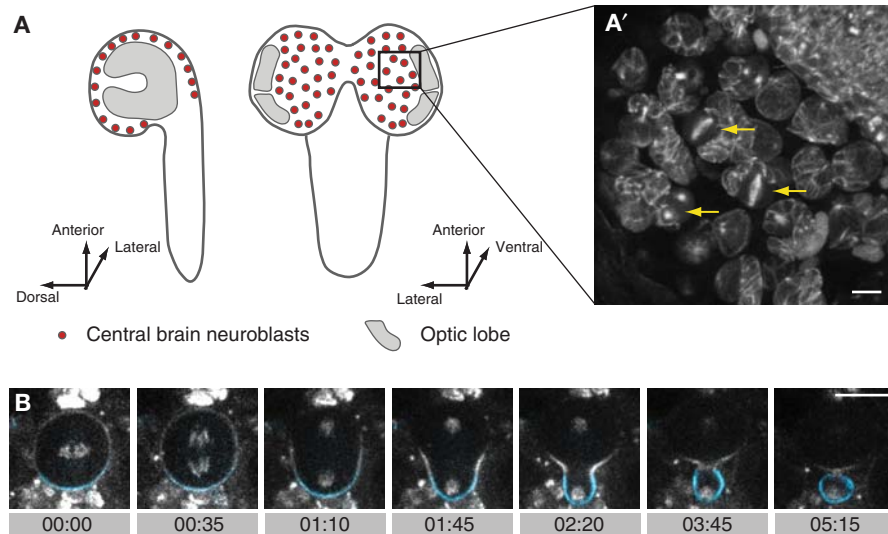


FIGURE 2. Live imaging third-instar larval neuroblasts. (A) Side- and dorsal-view schematics of third-instar larval brain and ventral nerve cord. Neuroblasts (red circles) are located close to the surface. (A') Snapshot from a time-lapse recording of dividing third-instar larval neuroblasts (from the boxed region in A). Mitotic neuroblasts (yellow arrows) are labeled with a microtubule binding protein (Jupiter) tagged with GFP using the G147 protein trap line (Morin et al. 2001). (B) Image sequence of a third-instar wild-type neuroblast expressing *UASHis2A::mRFP1* (Emery et al. 2005) as a DNA marker (gray), *UAS-Mira::GFP* (Cabernard and Doe 2009) (driven with *worniu-gal4* [Albertson and Doe 2003]) as a marker for basal cortex (blue), and *sqh::cherry* (Martin et al. 2009) controlled by the endogenous *sqh* promoter as a cleavage furrow marker (gray). Scale bars, 10 μ m. Time stamp, min:sec.

Ideally, live imaging is best performed in the intact animal in which neuroblasts are exposed to the correct spatial and temporal signaling inputs. Unfortunately, this is currently only possible for embryonic neuroblasts (Kaltschmidt et al. 2000). However, because embryonic neuroblasts are located relatively deep within the embryo, the signal-to-noise ratio can be low. One solution to this problem is to establish a primary embryonic neuroblast culture and to image isolated neuroblasts (Siegrist and Doe 2006; Broadus and Doe 1997). However, results derived from such cultures should be interpreted

TABLE 1. Fusion lines

Line	Structure to label	Fusion tag	Promotor/enhancer	Reference
<i>His2AvD::GFP</i>	DNA	GFP	Endogenous	Clarkson and Saint 1999
<i>UAS-His2A::mRFP1</i>	DNA	mRFP1	UAS	Emery et al. 2005
<i>G147</i>	Mitotic spindle	GFP	Endogenous	Morin et al. 2001
<i>UAS-Cherry::Jupiter</i>	Mitotic spindle	mCherry	UAS	Cabernard and Doe 2009
<i>UAS-mCherry::α-tubulin</i>	Mitotic spindle	mCherry	UAS	Rusan and Peifer 2007
<i>Baz::GFP</i>	Bazooka/apical crescent	GFP	Endogenous	Buszczak et al. 2007
<i>Pins::YFP</i>	Pins/apical crescent	YFP	Polyubiquitin	David et al. 2005
<i>UAS-GFP::Mira</i>	Miranda/basal crescent	GFP	UAS	Cabernard and Doe 2009
<i>UAS-Cherry::Mira</i>	Miranda/basal crescent	Cherry	UAS	Cabernard and Doe 2009
<i>UAS-Numb::GFP</i>	Numb/basal crescent	GFP	UAS	Roegiers et al. 2001
<i>UAS-Pon::mRFP1</i>	Pon/basal crescent	mRFP1	UAS	Emery et al. 2005
<i>Sqh::GFP</i>	Cleavage furrow	GFP	Endogenous	Royou et al. 2002
<i>Sqh::Cherry</i>	Cleavage furrow	mCherry	Endogenous	Martin et al. 2009
<i>UAS-actin::GFP</i>	Actin	GFP	UAS	Jacinto et al. 2000
<i>UAS-EB1::GFP</i>	Microtubule + ends	GFP	UAS	Rusan and Peifer 2007
<i>UAS-GFP::Cnn</i>	Centrosomes	GFP	UAS	Megraw et al. 2002
<i>Polo::GFP</i>	Centrosomes, kinetochores	GFP	Endogenous	Buszczak et al. 2007
<i>GFP::PACT</i>	Centrioles	GFP	Endogenous	Martinez-Campos et al. 2004
<i>Sas6::Cherry</i>	Centrioles	mCherry	Endogenous	Rusan and Peifer 2007
<i>YFP::asl</i>	Centrioles	YFP	Polyubiquitin	Rebollo et al. 2007

TABLE 2. Neuroblast Gal4 driver lines

Driver line	Enhancer/promotor	Reference
<i>Ase-Gal4</i>	<i>asense</i>	Zhu et al. 2006
<i>Wor-Gal4</i>	<i>wormiu</i>	Albertson and Doe 2003
<i>1407-Gal4</i>	<i>inscuteable</i>	Broadie et al. 1995

carefully. For example, spindle orientation differs between isolated embryonic neuroblasts clustered with epithelial cells versus fully isolated neuroblasts (Siegrist and Doe 2006). Because neuroblasts in larval brain explants are still in immediate contact with the same cells as in vivo (e.g., glia and ganglion mother cells; Siller et al. 2005), it is reasonable to assume that the imaged neuroblasts somewhat reflect the in vivo situation. Control experiments have confirmed this assumption: Bromodeoxyuridine incorporation experiments on intact larvae show a neuroblast cell-cycle time between 1 and 2 h (Truman et al. 1993); the same cell-cycle time is seen during long-term live imaging of neuroblasts in explanted brains (Cabernard and Doe 2009; C Cabernard, CQ Doe, unpubl.).

The method described here has been used to record the consequences of spindle orientation defects in mutant third-instar larval neuroblasts with regard to neuroblast cell cycle, polarity marker distribution, and self-renewal (Lee et al. 2006; Cabernard and Doe 2009). Other examples of live neuroblast studies include the analysis of neuroblast spindle rotation in embryos (Kaltschmidt et al. 2000), the neuroblast centrosome cycle (Rusan and Peifer 2007), neuroblast spindle pole movements (Siller and Doe 2008), and spindle orientation (Siller et al. 2006). Improvements in live imaging techniques have made it possible to reliably image neuroblasts in brain explants (Siller et al. 2005). Furthermore, several studies have taken advantage of embryonic primary neuroblast cultures to image isolated neuroblasts with or without adjacent tissue (Siegrist and Doe 2006; Rebollo et al. 2007). Recently, we have imaged third-instar larval neuroblasts for up to 20 h, which allowed recording of several subsequent neuroblast divisions (Lee et al. 2006; Cabernard and Doe 2009).

ACKNOWLEDGMENTS

We thank Karsten Siller and Sarah Siegrist for their pioneering work on neuroblast live imaging. We also thank Dan Graham for building and maintaining our imaging-analysis computer. This work was supported by HHMI (CQD) and the American Heart Association (CC).

REFERENCES

- Albertson R, Doe CQ. 2003. Dlg, Scrib and Lgl regulate neuroblast cell size and mitotic spindle asymmetry. *Nat Cell Biol* 5: 166–170.
- Brand AH, Perrimon N. 1993. Targeted gene expression as a means of altering cell fates and generating dominant phenotypes. *Development* 118: 401–415.
- Britton JS, Edgar BA. 1998. Environmental control of the cell cycle in *Drosophila*: Nutrition activates mitotic and endoreplicative cells by distinct mechanisms. *Development* 125: 2149–2158.
- Broadie K, Prokop A, Bellen HJ, O’Kane CJ, Schulze KL, Sweeney ST. 1995. Syntaxin and synaptobrevin function downstream of vesicle docking in *Drosophila*. *Neuron* 15: 663–673.
- Broadus J, Doe CQ. 1997. Extrinsic cues, intrinsic cues and microfilaments regulate asymmetric protein localization in *Drosophila* neuroblasts. *Curr Biol* 7: 827–835.
- Buszczak M, Paterno S, Lighthouse D, Bachman J, Planck J, Owen S, Skora AD, Nystul TG, Ohlstein B, Allen A, et al. 2007. The Carnegie protein trap library: A versatile tool for *Drosophila* developmental studies. *Genetics* 175: 1505–1531.
- Cabernard C, Doe CQ. 2009. Apical/basal spindle orientation is required for neuroblast homeostasis and neuronal differentiation in *Drosophila*. *Dev Cell* 17: 134–141.
- Clarkson M, Saint R. 1999. A *His2AvDGFP* fusion gene complements a lethal *His2AvD* mutant allele and provides an in vivo marker for *Drosophila* chromosome behavior. *DNA Cell Biol* 18: 457–462.
- David NB, Martin CA, Segalen M, Rosenfeld F, Schweisguth F, Bellaïche Y. 2005. *Drosophila* Ric-8 regulates G α i cortical localization to promote G α i-dependent planar orientation of the mitotic spindle during asymmetric cell division. *Nat Cell Biol* 7: 1083–1090.
- Emery G, Hutterer A, Berdnik D, Mayer B, Wirtz-Peitz F, Gaitan MG, Knoblich JA. 2005. Asymmetric Rab 11 endosomes regulate delta recycling and specify cell fate in the *Drosophila* nervous system. *Cell* 122: 763–773.
- Gao G, McMahon C, Chen J, Rong YS. 2008. A powerful method combining homologous recombination and site-specific recombination for targeted mutagenesis in *Drosophila*. *Proc Natl Acad Sci* 105: 13999–14004.
- Jacinto A, Wood W, Balayo T, Turmaine M, Martinez-Arias A, Martin P. 2000. Dynamic actin-based epithelial adhesion and cell matching during *Drosophila* dorsal closure. *Curr Biol* 10: 1420–1426.
- Kaltschmidt JA, Davidson CM, Brown NH, Brand AH. 2000. Rotation and asymmetry of the mitotic spindle direct asymmetric cell division in the developing central nervous system. *Nat Cell Biol* 2: 7–12.

- Karpova N, Bobinac Y, Foulx S, Huitorel P, Debec A. 2006. Jupiter, a new *Drosophila* protein associated with microtubules. *Cell Motil Cytoskeleton* 63: 301–312.
- Kiehart DP, Montague RA, Rickoll WL, Foard D, Thomas GH. 1994. High-resolution microscopic methods for the analysis of cellular movements in *Drosophila* embryos. *Methods Cell Biol* 44: 507–532.
- Lee C-Y, Andersen RO, Cabernard C, Manning L, Tran KD, Lanskey MJ, Bashirullah A, Doe CQ. 2006. *Drosophila* Aurora-A kinase inhibits neuroblast self-renewal by regulating aPKC/Numb cortical polarity and spindle orientation. *Genes Dev* 20: 3464–3474.
- Martin AC, Kaschube M, Wieschaus EF. 2009. Pulsed contractions of an actin–myosin network drive apical constriction. *Nature* 457: 495–499.
- Martinez-Campos M, Basto R, Baker J, Kernan M, Raff JW. 2004. The *Drosophila* pericentriolar-like protein is essential for cilia/flagella function, but appears to be dispensable for mitosis. *J Cell Biol* 165: 673–683.
- Megraw TL, Kilaru S, Turner FR, Kaufman TC. 2002. The centrosome is a dynamic structure that ejects PCM flares. *J Cell Sci* 115: 4707–4718.
- Morin X, Daneman R, Zavortink M, Chia W. 2001. A protein trap strategy to detect GFP-tagged proteins expressed from their endogenous loci in *Drosophila*. *Proc Natl Acad Sci* 98: 15050–15055.
- Rebollo E, Sampaio P, Januschke J, Llamazares S, Varmark H, González C. 2007. Functionally unequal centrosomes drive spindle orientation in asymmetrically dividing *Drosophila* neural stem cells. *Dev Cell* 12: 467–474.
- Roegiers F, Younger-Shepherd S, Jan LY, Jan YN. 2001. Two types of asymmetric divisions in the *Drosophila* sensory organ precursor cell lineage. *Nat Cell Biol* 3: 58–67.
- Royou A, Sullivan W, Karess R. 2002. Cortical recruitment of nonmuscle myosin II in early syncytial *Drosophila* embryos: Its role in nuclear axial expansion and its regulation by Cdc2 activity. *J Cell Biol* 158: 127–137.
- Rusan NM, Peifer M. 2007. A role for a novel centrosome cycle in asymmetric cell division. *J Cell Biol* 177: 13–20.
- Siegrist SE, Doe CQ. 2006. Extrinsic cues orient the cell division axis in *Drosophila* embryonic neuroblasts. *Development* 133: 529–536.
- Siller KH, Doe CQ. 2008. Lis1/dynactin regulates metaphase spindle orientation in *Drosophila* neuroblasts. *Dev Biol* 319: 1–9.
- Siller KH, Serr M, Steward R, Hays TS, Doe CQ. 2005. Live imaging of *Drosophila* brain neuroblasts reveals a role for Lis1/dynactin in spindle assembly and mitotic checkpoint control. *Mol Biol Cell* 16: 5127–5140.
- Siller KH, Cabernard C, Doe CQ. 2006. The NuMA-related Mud protein binds Pins and regulates spindle orientation in *Drosophila* neuroblasts. *Nat Cell Biol* 8: 594–600.
- Truman JW, Taylor BJ, Awad TA. 1993. Formation of the adult nervous system. In *The development of Drosophila melanogaster* (ed. Bate M, Martinez Arias A.), pp 1245–1275. Cold Spring Harbor Laboratory Press, Cold Spring Harbor, NY.
- Venken KJT, He Y, Hoskins RA, Bellen HJ. 2006. P[acman]: A BAC transgenic platform for targeted insertion of large DNA fragments in *D. melanogaster*. *Science* 314: 1747–1751.
- Venken KJT, Carlson JW, Schulze KL, Pan H, He Y, Spokony R, Wan KH, Koriabine M, de Jong PJ, White KP, et al. 2009. Versatile P[acman] BAC libraries for transgenesis studies in *Drosophila melanogaster*. *Nat Methods* 6: 431–434.
- Zhu S, Lin S, Kao CF, Awasaki T, Chiang AS, Lee T. 2006. Gradients of the *Drosophila* Chinmo BTB-zinc finger protein govern neuronal temporal identity. *Cell* 127: 409–422.